APPLIED ORGANOMETALLIC CHEMISTRY
Appl. Organometal. Chem. 2005; **19**: 363–371
Published online in Wiley InterScience (www.interscience.wiley.com). DOI:10.1002/aoc.852

Experimental and *ab initio* structural study of the ketotin compounds, $X_3SnCR_2CH_2COMe$: crystal structures of $X_3SnCMe_2CH_2COMe$ (X = Cl and I)

Bruce F. Milne[1], Robson P. Pereira[2], Ana Maria Rocco[2], Janet M. S. Skakle[3], Anthony J. Travis[4], James L. Wardell[2]* and Solange M. S. V. Wardell[5]

[1]Rua Quinta da Comenda, 44–1 °F, Águas Santas 4425-179, Maia, Porto, Portugal
[2]Instituto de Química, Universidade Federal do Rio de Janeiro, Centro de Tecnologia, Bloco A, Cidade Universitária, 21945-970, Rio de Janeiro, RJ, Brazil
[3]Department of Chemistry, University of Aberdeen, Meston Walk, Old Aberdeen AB24 3UE, Scotland, UK
[4]The Rowett Research Institute, Greenburn Road, Bucksburn, Aberdeen AB21 9SB, Scotland, UK
[5]Far-Manguinhos, Fiocruz, Rua Sizenando Nabuco 100, Manguinhos, CEP 21041-250, Rio de Janeiro, RJ, Brazil

Received 25 August 2004; Revised 13 September 2004; Accepted 11 October 2004

The $MeCOCH_2CMe_2$ ligand in $X_3SnCMe_2CH_2COMe$ (2; X = halide) acts as a *C,O*-chelating group both in the solid state and in non-coordinating solutions. The intramolecular Sn–O bond lengths in trigonal bipyramidal 2 (X = Cl and I), as determined by X-ray crystallography, indicate that the stronger interaction occurs in 2 X = Cl. Comparisons with the Sn–O bond lengths in the estertin trihalides, $X_3SnCH_2CH_2CO_2R$ (1; R = Me), suggest that the latter form stronger chelates than do 2. In chlorocarbon solution, 2 (X = Cl, I) undergoes exchange reactions, as shown by NMR spectra, to give all possible halide derivatives, $\sum(Cl_nI_{3-n}SnCMe_2CH_2COMe)$ (n = 0–3). Various *ab initio* calculations on 2 and $X_3SnCH_2CH_2COMe$ (3) have been carried out. Comparisons of the theoretical and experimental structures of 2 for X = Cl or I are reported. Copyright © 2005 John Wiley & Sons, Ltd.

KEYWORDS: chelate complexes; organotin compounds; crystallography; ketotin compounds; *ab initio* calculations

INTRODUCTION

Functionally substituted organotin compounds, $X_3SnCR_2CH_2COY$ (**I**) and $X_2Sn(CR_2CH_2COY)_2$ (**II**) (X = halide, R = H or alkyl, Y = alkyl, aryl or alkoxy), are readily available from reactions, first reported in the 1970s,[1] of $R_2C{=}CHCOY$, HX and SnX_2 (for **I**) or tin (for **II**). Original interest with these compounds was primarily involved with their industrial potential as precursors of PVC stabilizers,[6] but also with some concern with their coordination chemistry. Although the potential for use of **I** and **II** in PVC stabilization has not been realized commercially, the interest in the coordination chemistry, generally of compounds containing $SnCR_2CH_2COY$ moieties, has been maintained over the succeeding decades; of particular interest has been the coordination modes of the CR_2CH_2COY ligands.[7–41]

The derivatives with ester groups, e.g. $X_3SnCH_2CH_2CO_2R$ (**1**) and $X_2Sn(CH_2CH_2CO_2R)_2$, are generally termed estertin compounds, and have been studied much more frequently[1–5,7–39] than have the keto-tin compounds, e.g. $X_3SnCMe_2CH_2COMe$ (**2**) and $X_2Sn(CMe_2CH_2COMe)_2$ (**4**).[1–5,40–42] Indeed, only a few reports concerning the structural chemistry of the keto compounds have been published.[40,41] Some of us have reported the crystal structures of **4** with $X_2 = Cl_2, I_2$ and dmit (dmit = 1, 3-dithiol-2-thione-4,5-dithiol) and made comparisons with those of related estertin derivatives, $X_2Sn(CH_2CH_2CO_2Me)_2$ (**5**).[40,41] Both sets of dihalides are six-coordinate species in the solid state and in chlorocarbon solvents, as consequences of both CMe_2CH_2COMe moieties acting as *C,O*-chelating ligands.

We now report the findings of a study of $X_3SnCMe_2CH_2COMe$ (**2**), which includes the X-ray structures of **2** with

*Correspondence to: James L. Wardell, Instituto de Química, Universidade Federal do Rio de Janeiro, Centro de Tecnologia, Bloco A, Cidade Universitária, 21945-970, Rio de Janeiro, RJ, Brazil.
E-mail: j.wardell@abdn.ac.uk
Contract/grant sponsor: CNPq.
Contract/grant sponsor: FUJB.

X = Cl and I and various *ab initio* calculations on **2** (X = Cl, Br, I and Me). Similar calculations on $Cl_3SnCH_2CH_2COMe$ (**3**) are also reported. Comparisons of the calculated and experimental data, where possible, are also made.

EXPERIMENTAL AND METHODS

General

Melting points were measured using a Kofler hot-stage microscope and were uncorrected. IR spectra were recorded on a Nicolet Magna-IR 760 instrument. NMR spectra were obtained on Bruker 250 MHz and Bruker 400 MHz instruments.

Anhydrous $SnCl_2$ was obtained from the dihydrate on treatment with acetic anhydride (two equivalents), under nitrogen, followed by washing with small quantities of anhydrous ether and drying in vacuum.

Synthesis

Compound **2** *(X = Cl)*

To a suspension of anhydrous $SnCl_2$ (19.0 g, 0.1 mol) in dry Et_2O (30 ml) and mesityl oxide (10 g, 0.1 mol), cooled in an icebath, was slowly passed gaseous HCl until a homogeneous solution was obtained. The reaction mixture was stirred at room temperature for 1 h, and all volatiles were removed to leave an oily solid. The targeted product was initially heavily contaminated with a dark, non-volatile oily co-product, which was only removed after several recrystallizations from CH_2Cl_2–hexane; m.p. 124–125 °C (lit. value:[1]: 123 °C).

^{1}H NMR ($CDCl_3$, 250 MHz) δ: 1.47 (s, 6H, $J^{119,117}$Sn–^{1}H = 204.5, 195.3 Hz, Me_2C), 2.48 (s, 3H, MeCO), 3.05 (s, 2H, $J^{119,117}$Sn–^{1}H = 206.6, 197.5 Hz, CH_2).

^{119}Sn ($CDCl_3$, 93.3 Hz) δ: −135.4.

IR (CsI, cm^{-1}), ν: 2974, 2952, 2916, 2874, 1662, 1461, 1445, 1404, 1391, 1371, 1335, 1241, 1210, 1139, 1118, 1022, 998, 966, 837, 805, 606, 499, 450, 380, 354, 317, 264, 170.

Chem. Anal. Found: C, 22.3 H, 3.1. Calc. for $C_6H_{11}Cl_3OSn$: C, 22.2; H, 3.4%.

Compound **2** *(X = I)*

To a solution of **2** (X = Cl; 3.24 g, 10 mmol) in Me_2CO (10 ml) was added a solution of NaI (8 g) in Me_2CO (40 ml). After stirring the reaction mixture for 2 h at room temperature, the mixture was filtered and the filtrate evaporated to leave a residue. This residue was extracted with $CHCl_3$ and the $CHCl_3$ extracts evaporated. The resulting residue was recrystallized from CH_2Cl_2–cyclohexane.

^{1}H NMR ($CDCl_3$, 250 MHz) δ: 1.08 (s, 6H, $J^{119,117}$Sn–^{1}H = 199.3, 190.9 Hz, Me_2C), 2.39 (s, 3H, MeCO), 2.60 (s, 2H, $J^{119,117}$Sn–^{1}H = 197.7, 189.5 Hz, CH_2).

^{119}Sn ($CDCl_3$, 93.3 Hz) δ: −545.5.

IR (CsI, cm^{-1}), ν: 2961, 2937, 2905, 2861, 1668, 1451, 1441, 1384, 1369, 1332, 1244, 1208, 1181, 1108, 1016, 995, 964, 795, 618, 495, 445, 375, 322, 279, 251, 229, 194, 172, 153.

Chem. Anal. Found: C, 12.2; H, 2.1. Calc. for $C_6H_{11}I_3OSn$: C, 12.0; H, 1.9%.

Crystallography

Low temperature intensity data for **2** (X = Cl) were collected on a Nonius KappaCCD area detector system by the EPSRC X-ray crystallographic service at the University of Southampton, UK. The entire process of data collection, cell refinement and data reduction was accomplished by means of the programs DENZO[42] and COLLECT.[43] Correction for absorption was achieved by a semi-empirical method based upon the variation in intensity of equivalent reflections with the program SORTAV.[44,45] Room-temperature intensity data for **2** (Cl or I) were collected on a Bruker SMART CCD area detector diffractometer. Data collection, cell refinement and data collection were achieved using SAINT software[46] and absorption correction achieved using SADABS.[46]

The structures were solved by direct methods in SHELXS-97[47] within the OSCAIL suite of programs[48] and refined in SHELXL-97.[49] In the final stages of refinement the hydrogen atoms were placed in calculated positions and refined with a riding model. PLATON was used for data analysis.[50] The program ORTEP-3 for Windows was used to obtain the figures.[51]

Crystal data for **2** *(X = Cl) at 120(2) K*

Colourless crystal 0.49 × 0.27 × 0.22 mm^3. Formula: $C_6H_{11}Cl_3OSn$; M = 324.19; orthorhombic, *Pbca*, a = 12.7225(2) Å, b = 13.7658(2) Å, c = 12.8638(2) Å, Z = 8, V = 2252.91(6) Å^3, 2573 independent reflections (R_{int} = 0.0495), 2474 observed reflections ($I > 2\sigma(I)$); parameters refined: 104; number of restraints: 0; $R(F)$: 0.031 (obs. data); wR (F^2) = 0.083 (all data), $\Delta\rho_{max}$ = 1.34 e$^-$ Å^{-3}. CCDC deposition no: 245 829.

Crystal data for **2** *(X = Cl) at 290(2) K*

Colourless crystal 0.49 × 0.27 × 0.22 mm^3. Formula: $C_6H_{11}Cl_3OSn$; M = 324.19; orthorhombic, *Pbca*, a = 12.8973(13) Å, b = 13.9200(15) Å, c = 12.9363(14) Å, β = 97.204(2)°, Z = 8, V = 2322.5(4) Å^3, 3391 independent reflections (R_{int} = 0.0217), 2557 observed reflections ($I > 2\sigma(I)$); parameters refined: 104; number of restraints: 0; $R(F)$: 0.026 (obs data); wR (F^2) = 0.070 (all data), $\Delta\rho_{max}$ = 0.56 e$^-$ Å^{-3}. CCDC deposition no: 245 828.

Crystal data for **2** *(X = I) at 291(2) K*

Pale yellow crystal 0.42 × 0.18 × 0.10 mm^3. Formula: $C_6H_{11}I_3OSn$; M = 598.54; monoclinic, *I2/a*; a = 26.189(3) Å, b = 7.7580(8) Å, c = 27.369(3) Å, Z = 8, V = 5516.8(10) Å^3, 10 254 independent reflections (R_{int} = 0.0340), 5949 observed reflections ($I > 2\sigma(I)$); parameters refined: 206; number of restraints: 0; $R(F)$: 0.036 (obs data); $wR(F^2)$ = 0.090 (all data), $\Delta\rho_{max}$ = 1.14 e$^-$ Å^{-3}. CCDC deposition no: 245 830.

Ab initio calculations

All geometries were fully optimized by the analytical gradient method utilizing GAMESS[52] in the restricted Hartree–Fock

(RHF) level with 4-31G, 6-31G and 6-31G(d,p) basis sets for carbon, oxygen, hydrogen and chlorine and the SBKJC effective core potentials for tin, bromine and iodine. Subsequently, geometries were also optimized using the LANL2DZ(d,p) effective core potential basis set on tin and halides and the 6-31G(d,p) basis set on hydrogen, carbon and oxygen.

In order to evaluate the effect on the structures of the ketotins of including electron correlation, calculations were performed at the MP2 and DFT (B3LYP) levels of theory. As it was felt that the SBKJC basis was rather inflexible for use with correlation treatments, the LANL2DZ(d,p) effective core potential set including diffuse/polarization functions was obtained from the EMSL basis set library (see Acknowledgements) and used for tin and all halides. The 6-31G(d,p) set provided internally with GAMESS was used for hydrogen, carbon and oxygen.

Geometries were optimized first at the RHF level using this basis set and subsequent optimizations at the MP2 and B3LYP levels were begun from the RHF minimum-energy structures. At the end of the optimizations a harmonic vibrational analysis was performed on each structure and the force-constant matrix obtained and decomposed in terms of a system of delocalized internal coordinate[53] defining the bonds, angles and torsions of the molecules. In this way, the intrinsic vibrational frequencies[54] relating to these molecular degrees of freedom were obtained.

All calculations in which the LANL2DZ(d,p) basis was employed (RHF, MP2 and B3LYP) were performed with the parallel GAMESS-US code[52] (14 January 2003 version) on the 32-node Athlon 2600+ Linux cluster at the Rowett Research Institute.

Force constants

Force constants were obtained for **2** (X = Cl, Br, I and Me) by performing a vibrational analysis of the molecules using an internal coordinate system rather than Cartesians. This coordinate system defined the molecule's degrees of freedom in terms of 3N-6 stretches and bends (angles and torsions), making it simpler to assign force constants to particular motions within the molecular force field. The vibrational spectra were then calculated utilizing the optimized geometries obtained in each case and the frequencies presented are unscaled.

For comparative purposes, the force constant for the C–C bond in ethane was calculated at the RHF/6-31G(d,p) level and found to be 4.213×10^{-3} Dyn $Å^{-1}$.

RESULTS AND DISCUSSION

Synthesis

The compound $Cl_3SnCMe_2CH_2COMe$ (**2**; X = Cl) was obtained from $Me_2C{=}CHCOMe$, HCl and anhydrous $SnCl_2$ in Et_2O, following the reported procedure.[1–5] Although the final yield of pure **2** (X = Cl) was low due to the difficulty of separating the product from other material, sufficient was obtained for subsequent study. An alternative procedure to **2** with X = Cl, using acetone instead of $Me_2C{=}CHCOMe$, has been reported,[55] but was not used here. Compound **2** (X = I) was achieved by halide exchange between **2** (X = Cl) and NaI in acetone solution at room temperature. The use of a two fold excess of NaI with short reaction times was sufficient to give complete halide exchange, as indicated by elemental analysis and by the X-ray diffraction study. Halide exchange with less than 90% conversion, giving $Cl_nI_{3-n}SnCMe_2CH_2COMe$ ($0 \le n \le 3$), can be detected by solution ^{119}Sn NMR spectroscopy, since chemical shifts for individual species, $Cl_nI_{3-n}SnCMe_2CH_2COMe$ (n an integer), can be observed; see later.

Solid state studies: X-ray crystallography

The X-ray crystal structure of **2** (X = I) was determined at 291(2) K, and that of **2** (X = Cl) was obtained both at 290(2) and 120(2) K, with the same basic structure for **2** (X = Cl) being obtained at the two temperatures. Both compounds **2** (X = Cl, I) exhibit Sn–O intramolecular coordination, resulting in chelated structures with trigonal bipyramidal geometries at tin with oxygen and a halide in axial sites; see Figures 1 and 2. As shown by the torsion angles, the chelate rings in **2** (X = Cl, I) have envelope shapes with flaps at the α carbon atoms, C1. Selected geometric parameters are displayed in Tables 1 and 2.

Two independent molecules, A and B, with similar geometries, are found in the asymmetric unit of **2** (X = I), with a significant difference being the chelate bite angles of 72.82(14) Å (molecule A) and 74.03(14) Å (molecule B). Of interest, the carbonyl oxygen atom in molecule A, but not that in molecule B, is involved in a short C(H)···O contact. Analysis of the data using PLATON[50] indicated that such interactions also occur in **2** (X = Cl). Such contacts involve the methyl of the COMe. The relevant distances

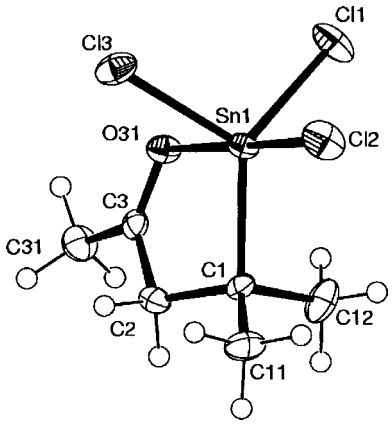

Figure 1. Atom arrangements and numbering scheme for **2** (X = Cl). Ellipsoids are shown at the 40% probability level, hydrogen atoms are shown as circles.

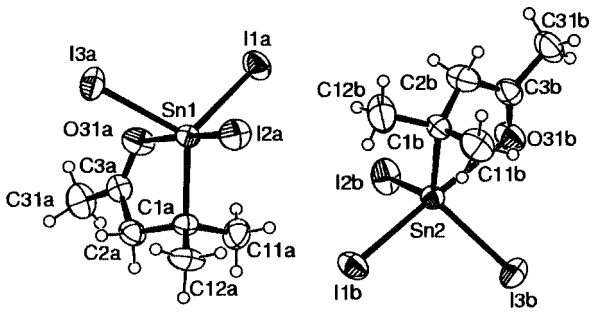

Figure 2. Atom arrangements and numbering scheme for the two independent molecules of **2** (X = I). Ellipsoids are shown at the 40% probability level; hydrogen atoms are shown as circles. Molecule 'A' is shown in the same orientation as that of Figure 1.

Table 1. Selected bond lengths (Å) and angles (°) for **2** (X = Cl)

	290(2) K	150(2) K
Sn1–C1	2.174(3)	2.173(3)
Sn1–Cl1	2.3246(9)	2.3287(7)
Sn1–Cl2	2.3287(9)	2.3377(6)
Sn1–Cl3	2.3789(9)	2.3865(7)
Sn1–O31	2.3926(19)	2.3887(17)
C3–O31	1.218(3)	1.228(3)
C1–Sn1–Cl1	123.14(8)	123.05(7)
C1–Sn1–Cl2	121.64(9)	121.73(8)
Cl1–Sn1–Cl2	106.47(5)	106.61(3)
C1–Sn1–Cl3	104.93(8)	104.97(7)
Cl1–Sn1–Cl3	97.78(4)	97.64(3)
Cl2–Sn1–Cl3	95.96(4)	95.81(3)
C1–Sn1–O31	75.36(9)	75.72(8)
Cl1–Sn1–O31	82.82(6)	82.52(5)
Cl2–Sn1–O31	83.07(6)	83.20(5)
Cl3–Sn1–O31	178.98(6)	179.00(5)
C3–O31–Sn1	111.47(18)	110.67(17)
C1–C2–C3–O31	−27.1(4)	−26.8(4)
Sn1–C1–C2–C3	40.6(3)	41.2(3)
O31–Sn1–C1–C2	−29.0(2)	−30.40(17)
C3–O31–Sn1–C1	18.4(2)	19.75(18)
C2–C3–O31–Sn1	−1.0(3)	−1.9(3)

Hydrogen bonding parameters, 120(2) K:

D–H···A	*d*(D–H)	*d*(H···A)	*d*(D···A)	<(D–H···A)
C(31)–H(31A)···O(31)^{i}	0.98	2.58	3.477(4)	153

Symmetry operations *i*: $-x+1, -y+1, -z+1$.

and angles, given in Tables 1 and 2, are all within the ranges accepted for weak hydrogen-bonding interactions;[56] however, the high mobility of methyl groups requires some caution in accepting that they participate in actual hydrogen bonding.

Two independent molecules were also found in the X-ray crystal structure determination of $I_3SnCH_2CH_2CO_2Me$ (**1**; X = I, R = Me).[36] However, in this case, there were more significant differences between the distorted trigonal bipyramidal geometries of the two molecules A′ and B′, as shown by the Sn–O bond lengths (2.459(8) Å and 2.631(8) Å respectively), the axial Sn–I bond lengths (2.7601(10) Å and 2.7188(9) Å respectively) and the chelate bite angles (76.5(3)° and 70.6(3)° respectively). Another major difference between molecules A′ and B′ of **1** (X = I, R = Me) is that an iodide of molecule A′ acts as an acceptor for two C–H···I intermolecular hydrogen bonds, whereas no corresponding interaction involves molecule B′. As pointed out by Tiekink and coworkers,[57] such intermolecular interactions and crystal packing effects have significant influences on geometric parameters.

An effect of changing the temperature of the data collection from 290 K to 120 K for **2** (X = Cl) was the increase in the Sn–Cl3$_{(axial)}$ bond length from 2.3789(9) to 2.3865(7) Å. However, the Sn–O31 bond length remained effectively unchanged over the two temperatures, the values being 2.3926(19) Å at 290 K and 2.3887(17) Å at 120 K. Comparison of the Sn–O bond lengths in **2** (X = Cl; 2.3926(19) Å) and **2** (X = I; 2.516(3) and 2.518(3) Å) at 290 K confirms that the stronger chelation occurs in the chloride. A similar comparison of the Sn–O bond lengths in **2** (X = Cl) and **1** (X = Cl, R = Me)[37–39] indicates that the stronger interaction occurs in the estertin **1** (X = Cl, R = Me). Owing to the very different Sn–O bond lengths (2.459(8) and 2.631(8) Å) in the two independent molecules of **1** (X = I, R = Me),[36] similar comparisons involving **2** (X = I) are not made.

As expected, the Sn–Cl$_{(equatorial)}$ bonds are shorter than the Sn–Cl$_{(axial)}$ bonds in **2** (X = Cl), and both are longer than Sn–Cl bonds in tetrahedral, i.e. molecular and non-aggregated $RSnCl_3$ compounds, e.g. R/*d*(Sn–Cl) = Me/2.307(16) Å,[58] η^1-C_5Ph_5/2.314(2) Å,[59] $(Me_2PhSi)_3C$/2.317(4) Å,[60] and ^{t}Bu/2.320(5) Å.[61] Similar situations occur with triiodides, as shown by Sn–I bond lengths of 2.6692(11) Å and 2.681 Å (mean) in $MeSnI_3$[62] and η^1-$C_5Me_5SnI_3$[63] respectively. Coordination of tin centres by internal donors in functionally substituted organotin trihalides generally results in similar lengthening of the Sn–Cl and Sn–I bonds, as shown for example by the estertins **1**[37–39] and **1** (X = I, R = Me).[36]

The Sn–O coordinations in solid **2** are also indicated by the ν(CO) values of 1670–1660 cm^{-1} in the IR spectra.

Solution studies: NMR spectra

The Sn–O coordination in **2** persists in non-coordinating solvents, such as chlorocarbons, as shown by the similar ν(CO) values to those found in the solid-state IR spectra and by the NMR spectra. For example, the $^2J(^{119}Sn-^1H)$ coupling constants for the Me_2C and CH_2 protons in **2** (X = Cl, 204.5 Hz and 206.6 Hz respectively) and **2** (X = I; 199.0 Hz and 197.7 Hz respectively) indicate coordination numbers greater than four

Table 2. Selected geometric parameters for **2** (X = I) at 291(2) K

Molecule A		Molecule B	
Sn1–C1a	2.206(4)	Sn2–C1b	2.194(4)
Sn1–I1a	2.7011(5)	Sn2–I2b	2.6926(5)
Sn1–I2a	2.7375(5)	Sn2–I1b	2.7449(5)
Sn1–I3a	2.7019(5)	Sn2–I3b	2.6940(5)
Sn1–O31a	2.516(3)	Sn2–O31b	2.518(3)
C3a–O31a	1.223(6)	C3b–O31b	1.195(6)
C1a–Sn1–I1a	119.17(12)	C1b–Sn2–I2b	116.56(12)
C1a–Sn1–I3a	119.92(12)	C1b–Sn2–I3b	121.63(12)
I1a–Sn1–I3a	110.439(16)	I3b–Sn2–I2b	111.522(18)
C1a–Sn1–I2a	105.35(11)	C1b–Sn2–I1b	105.08(12)
I1a–Sn1–I2a	99.946(16)	I1b–Sn2–I2b	99.909(16)
I3a–Sn1–I2a	96.855(16)	I1b–Sn2–I3b	97.034(16)
C1a–Sn1–O31a	72.82(14)	C1b–Sn2–O31b	74.03(14)
O31a–Sn1–I1a	84.28(8)	O31b–Sn2–I2b	83.94(9)
O31a–Sn1–I3a	81.01(9)	O31b–Sn2–I3b	80.31(9)
O31a–Sn1–I2a	175.74(8)	O31b–Sn2–I1b	175.96(9)
C2a–O31a–Sn1	109.5(3)	C2b–O31b–Sn2	110.3(3)
C1a–C2a–C3a–O31a	−24.8(6)	C1b–C2b–C3b–O31b	28.5(8)
Sn1–C1a–C2a–C3a	43.5(5)	Sn2–C1b–C2b–C3b	−39.0(6)
O31a–Sn1–C1a–C2a	−32.0(3)	O31b–Sn2–C1b–C2b	25.9(3)
C3a–O31a–Sn1–C1a	22.8(3)	C3b–O31b–Sn2–C1b	−14.4(4)
C2a–C3a–O31a–Sn1	−5.7(5)	C2b–C3b–O31b–Sn2	−2.8(6)

Hydrogen bonding parameters:

D–H···A	*d*(D–H)	*d*(H···A)	*d*(D···A)	<(D–H···A)
C(31B)–H(31E)···O(31a)^{i}	0.96	2.57	3.351(7)	139

Symmetry operation *i*: $-x+1/2, -y+1/2, -z+1/2$.

for tin. Exchange occurred between **2** (X = Cl) and **2** (X = I) in $CHCl_3$ solution to give all possible halides **2** ($X_3 = Cl_n I_{3-n}$: $n = 0$–3) as shown by ^{119}Sn NMR spectroscopy. Values of δ^{119}Sn obtained were: −135.4 (**2**: $X_3 = Cl_3$), −289.6 (**2**: $X_3 = Cl_2I$), −428.1 (**2**: $X_3 = ClI_2$), and −541.5 ppm (**2**: $X_3 = I_3$). For the mixed halides, only one chemical shift value was observed, despite the possibilities of isomeric trigonal bipyramidal structures, formed by the different halo groups occupying axial and equatorial positions.

Ab initio calculations

Values of selected geometric parameters for **2** and **3** are listed in Table 3 for the different levels and/or basis sets used in the present work and compared with the experimental ones for **2** (X = Cl, I). RHF calculations with the 6-31G(d,p) basis set exhibit the best results for the majority of the parameters considered. The combination of the DFT functional B3LYP with the effective core potential LANL2DZ seems to overestimate bond lengths involving tin, probably due to a different description of the electron–nucleus interaction compared with the SBKJC ECP.

It could be surprising, at a first examination, that the calculated geometries present such small deviations from the experimental ones for a given level of theory and basis set. However, an observing the crystal packing and the individuality of the molecules for **2** with X = Cl and X = I in the solid state, it is quite reasonable that these molecules behave like isolated molecular systems, which are exactly the simulated systems in the *ab initio* calculations. The absence of significant intermolecular interactions and the presence of strong intramolecular coordination (C═O···Sn) in these systems allows the calculation of each molecule as an isolated entity and hence representative of the molecular geometry in the solid state. Where interspecies interactions occur, as in $[NBu_4[Bi(dmit)_2]$,[6] the situation is quite different.

Geometrical parameters, calculated by each method, present coherent trends for both series (**2**: X = Cl, Br, I) and (**3**: X = Cl, Br, I). Calculated Sn–C bond lengths shows a slight increase in each series from X = Cl, Br and I, with generally longer Sn–C bond lengths for **2** than for **3**. Comparison of the calculated Sn–O and axial Sn–X bond lengths indicates slightly stronger intramolecular

Table 3. Comparison of selected calculated and experimental geometric data for **2** and **3**

		RHF					X-ray data	
	Parameter	6-31G(d,p)/ SBKJC[a]	6-31G(d,p)/ SBKJC[b]	6-31G(d,p), LANL2DZ	MP2, 6-31G(d,p), LANL2DZ	B3LYP, 6-31G(d,p), LANL2DZ	290 K	120 K
3 (X = Cl)	Sn–C	2.139	2.134	2.131	2.136	2.153		
	Sn–X (eq)	2.331	2.364	2.313	2.315	2.349		
	Sn–X (ax)	2.376	2.408	2.354	2.347	2.382		
	Sn–O	2.405	2.430	2.427	2.432	2.415		
	C═O	1.204	1.204	1.205	1.239	1.230		
	O–Sn–C	75.3	74.0	73.8	74.3	75.1		
	C–C–C–Sn	−0.64	−29.2	−29.5	−33.9	−25.1		
2 (X = Cl)								
	Sn–C	2.176	2.171	2.169	2.166	2.2002	2.174(3)	2.173(3)
	Sn–X (eq)	2.338	2.377	2.318	2.318	2.3538	2.3266(av)	2.3322(av)
	Sn–X (ax)	2.389	2.425	2.36	2.352	2.3934	2.3789(9)	2.3865(7)
	Sn–O	2.382	2.398	2.429	2.439	2.4098	2.3926(19)	2.3887(19)
	C═O	1.204	1.206	1.205	1.239	1.2311	1.218(3)	1.228(3)
	O–Sn–C	77.2	75.1	74.3	74.7	79.98	75.36(9)	75.72(8)
	C–C–C–Sn	−0.86	−37.2	−38.5	−41.7	−31.36	40.6(3)	41.2(3)
3 (X = Br)	Sn–C	2.139	2.136	2.138	2.144	2.161		
	Sn–X (eq)	2.519	2.519	2.484	2.487	2.521		
	Sn–X (ax)	2.577	2.577	2.529	2.522	2.557		
	Sn–O	2.498	2.528	2.509	2.48	2.464		
	C═O	1.205	1.205	1.203	1.238	1.229		
	O–Sn–C	71.3	71.4	72.1	73.2	74.2		
	C–C–C–Sn	−0.61	−38.4	−34.0	−36.6	−27.3		
2 (X = Br)	Sn–C	2.186	2.183	2.181	2.178	2.216		
	Sn–X (eq)	2.527	2.525	2.490	2.491	2.527		
	Sn–X (ax)	2.59	2.579	2.536	2.528	2.572		
	Sn–O	2.375	2.472	2.500	2.483	2.436		
	C═O	1.205	1.204	1.204	1.239	1.230		
	O–Sn–C	77.2	73.7	72.9	73.7	75.3		
	C–C–C–Sn	−0.80	−39.8	−40.9	−43.6	−32.6		
3 (X = I)	Sn–C	2.153	2.146	2.147	2.153	2.169		
	Sn–X (eq)	2.733	2.73	2.700	2.705	2.734		
	Sn–X (ax)	2.802	2.787	2.747	2.743	2.775		
	Sn–O	2.466	2.607	2.596	2.522	2.517		
	C═O	1.203	1.200	1.202	1.237	1.229		
	O–Sn–C	74.1	70.4	80.4	72.3	82.9		
	C–C–C–Sn	−0.851	−37.3	−37.6	−38.8	−33.6		
2 (X = I)							Two independent molecules	
	Sn–C	2.202	2.198	2.197	2.194	2.232	2.206(4)	2.194(4)
	Sn–X (eq)	2.743	2.734	2.708	2.710	2.742	2.7015(av)	2.6933(av)
	Sn–X (ax)	2.820	2.799	2.758	2.751	2.794	2.7375(5)	2.7449(5)
	Sn–O	2.429	2.584	2.573	2.521	2.473	2.516(3)	2.518(3)
	C═O	1.203	1.201	1.202	1.238	1.230	1.223(6)	1.195(6)
	O–Sn–C	76.1	71.7	71.7	73.0	74.2	72.82(14)	74.03(14)
	C–C–C–Sn	−1.140	−43.0	−43.0	−44.4	−36.9	43.5(5)	−39.0(6)

[a] Flat chelate structures.
[b] 'Envelope' chelate structures.

Table 4. Calculated harmonic force constants and frequencies for **2** and **3**

		RHF		MP2		B3LYP	
Coordinate	Compound	HFC[a]	IHVF[b]	HFC[a]	IHVF[b]	HFC[a]	IHVF[b]
Sn–C	**2**: X = Cl	1.429	444.8	1.460	469.5	1.132	411.7
	2: X = Br	1.339	430.7	1.368	454.2	1.051	394.9
	2: X = I	1.233	413.2	1.252	434.8	0.949	376.9
	3: X = Cl	1.737	487.1	1.713	508.5	1.450	466.1
	3: X = Br	1.662	479.6	1.650	499.0	1.380	454.7
	3: X = I	1.539	469.9	1.578	488.0	1.325	445.6
Sn–X (eq.)	**2**: X = Cl	1.716	309.4	1.915	341.2	1.785	328.2
	2: X = Br	1.365	208.2	1.529	230.0	1.443	222.4
	2: X = I	1.269	176.7	1.348	189.7	0.939	157.7
	3: X = Cl	2.027	336.3	2.181	363.8	1.817	331.2
	3: X = Br	1.655	229.2	1.767	247.5	1.475	225.0
	3: X = I	1.314	178.9	1.374	191.7	1.010	163.7
Sn–X (ax.)	**2**: X = Cl	1.991	333.3	2.151	361.6	1.549	305.8
	2: X = Br	1.616	226.5	1.757	245.2	1.221	204.8
	2: X = I	1.056	160.8	1.169	176.6	1.130	173.8
	3: X = Cl	1.769	314.3	1.967	345.8	1.630	313.8
	3: X = Br	1.616	211.9	1.574	233.4	1.300	211.3
	3: X = I	1.056	164.5	1.212	179.8	1.163	175.6
Sn–O	**2**: X = Cl	0.500	231.3	0.611	267.0	0.572	257.4
	2: X = Br	0.420	212.1	0.551	253.6	0.541	250.5
	2: X = I	0.360	196.2	0.502	242.0	0.482	236.2
	3: X = Cl	0.511	233.9	0.625	270.0	0.558	254.1
	3: X = Br	0.424	212.9	0.558	255.0	0.485	234.1
	3: X = I	0.360	196.4	0.507	243.3	0.414	218.9
C═O	**2**: X = Cl	12.289	1645.4	10.656	1599.6	10.712	1598.0
	2: X = Br	12.422	1654.3	10.686	1601.8	10.753	1601.1
	2: X = I	12.541	1662.2	10.703	1603.1	10.766	1602.0
	3: X = Cl	12.299	1646.1	10.695	1602.5	10.740	1600.1
	3: X = Br	12.422	1655.6	10.716	1604.1	10.815	1605.7
	3: X = I	12.541	1664.3	10.726	1604.9	10.832	1607.0
O–Sn–C	**2**: X = Cl		236.6		232.1		237.8
	2: X = Br		229.6		227.6		234.9
	2: X = I		222.5		224.0		233.0
	3: X = Cl		245.9		241.9		243.9
	3: X = Br		237.9		237.3		231.4
	3: X = I		229.8		233.3		227.6
C–C–C–Sn	**2**: X = Cl		446.3		443.3		420.9
	2: X = Br		447.1		445.2		421.0
	2: X = I		448.6		446.5		423.0
	3: X = Cl		445.6		441.5		420.6
	3: X = Br		446.6		442.2		415.7
	3: X = I		447.3		444.3		424.6

[a] Harmonic force constant.
[b] Intrinsic harmonic vibrational frequency.

coordination in compounds **3** compared with **2**, for most calculation methods.

From Table 4 it can be seen that the force constant associated with stretching of the Sn–O bond is reduced and the Sn–O distance is increased as X becomes larger, suggesting that larger halides weaken the Sn–O interaction. Lowering of the Sn–O force constant is accompanied by an increase in the C═O stretching force constant and slight decreases in the C═O distance, suggesting that this bond might be absorbing charge density released from the Sn–O

region due to decreases in the electron-withdrawing abilities of X.

Owing to the shape of the potential energy surface (PES) of these systems, flat chelate ring structures may be found instead of envelopes, depending on the calculation used (both basis sets and method). These flat structures represent local minima on the PES and may be interpreted as possible structures in equilibrium with the envelope structures, depending on the energy given to the system. For the lower levels of calculations (RHF with N-31G and 6-31G(d,p) basis sets with SBKJC ECP on tin), these flat structures are the result of the geometry search, but envelope structures are found for MP2, B3LYP and RHF/6-31G(d,p)/LANL2DZ. The shape of the PES described with the different methods and basis sets is not exactly the same, and the observed qualitatively different final structures are a clear effect of this.

A suitable choice of individual molecules or other representative units of a material is required in performing high-level wave-function quantum-chemical methods calculations. In the cases of **2** and **3**, owing to the lack of strong intermolecular interactions and the presence of strong intramolecular coordination, calculations based on individual molecules are a reasonable approach to the description of the actual system. The weak intermolecular interactions in **2** are clearly too insignificant to invalidate their absence from the theoretical treatments. However, when crystal packing effects and intermolecular interactions are important, then different approaches are required in order to describe the contribution of these interactions to the formation of the solid. Bonds, somewhat longer than the sum of the covalent radii, but well within the van der Waals radii sum, can usually be adequately described with the implementation of diffuse and highly flexible functions to the basis set. In the present case, however, the diffuse functions cover the intramolecular coordination observed in the real systems.

Acknowledgements

We are indebted to the EPSRC for the use of both the Chemical Database Service at Daresbury, UK, primarily for access to the Cambridge Structural Database, and the X-ray service at the University of Southampton, UK, for data collection for **2** (X = Cl) at 120 K. We thank CNPq and FUJB, Brazil, for financial support.

Basis sets were obtained from the Extensible Computational Chemistry Environment Basis Set Database, Version 02/25/04, as developed and distributed by the Molecular Science Computing Facility, Environmental and Molecular Sciences Laboratory which is part of the Pacific Northwest Laboratory, PO Box 999, Richland, WA 99352, USA, and funded by the US Department of Energy. The Pacific Northwest Laboratory is a multi-programme laboratory operated by Battelle Memorial Institute for the US Department of Energy under contract DE-AC06-76RLO 1830. Contact David Feller or Karen Schuchardt for further information.

REFERENCES

1. Hutton RE, Oakes V. *Adv. Chem. Ser.* 1976; **157**: 123.
2. Hutton RE, Burley JW, Oakes V. *J. Organometal. Chem.* 1978; **156**: 369.
3. Burley JW, Hope O, Hutton RE, Groenenboom CJ. *J. Organometal. Chem.* 1979; **170**: 21.
4. Burley JW, Hutton RE, Jolley MRJ, Groenenboom CJ. *J. Organometal. Chem.* 1983; **251**: 189.
5. Burley JW, Hutton RE. *J. Organometal. Chem.* 1982; **216**: 165.
6. Lanigen D, Weinberg EL. *Adv. Chem. Ser.* 1976; **157**: 134.
7. Ng SW, Kumar Das VG. *Acta Crystallogr. Sect C* 1995; **51**: 2492.
8. Ng SW. *Acta Crystallogr. Sect C* 1993; **49**: 753.
9. Ng SW, Wei C, Kumar Das VG, Jameson GB, Butcher RJ. *J. Organometal. Chem.* 1989; **365**: 75.
10. Ng SW, Chen W, Kumar Das VG, Charland JP, Smith FE. *J. Organometal. Chem.* 1989; **364**: 343.
11. Li ZF, Wang SW, Tian XY, Fu FX, Pan HD. *Chin. J. Org. Chem.* 2000; **20**: 206.
12. Li ZF, Fu FX, Pan HD, Xing Y, Lin YH. *Acta Chin. Sin.* 1999; **57**: 820.
13. Gielen M, Huade P, Tiekink ERT. *Bull. Soc. Chim. Belg.* 1993; **102**: 447.
14. Jung OS, Jeong JH, Sohn YS. *Organometallics* 1991; **10**: 761, 2217.
15. Jung OS, Jeong JH, Sohn YS. *J. Organometal. Chem.* 1990; **399**: 235.
16. Jung OS, Jeong JH, Sohn YS. *J. Organometal. Chem.* 1990; **397**: 17.
17. Jung OS, Jeong JH, Sohn YS. *Acta Crystallogr. Sect C* 1990; **46**: 31.
18. Jung OS, Jeong JH, Sohn YS. *Polyhedron* 1989; **8**: 1413, 2557.
19. Balasubramanian R, Chohan ZH, Doidge-Harrison SMSV, Howie RA, Wardell JL. *Polyhedron* 1997; **16**: 4283.
20. Chohan ZH, Howie RA, Wardell JL, Wilkens R, Doidge-Harrison SMSV. *Polyhedron* 1997; **16**: 2689.
21. Buchanan H, Howie RA, Khan A, Spencer GM, Wardell JL, Aupers JH. *J. Chem. Soc. Dalton Trans.* 1996; 541.
22. Harston P, Howie RA, McQuillan GP, Wardell JL, Zanetti E, Doidge-Harrison SMSV, Stewart NS, Cox PJ. *Polyhedron* 1991; **10**: 1085.
23. Paterson ES, Wardell JL. *J. Organometal. Chem.* 1984; **273**: 313.
24. Maughan D, Wardell JL, Burley JW. *J. Organometal. Chem.* 1981; **212**: 59.
25. Li ZF, Wang SW, Wang YX, Fu FX. *Chem. J. Chin. Univ.-Chin.* 2002; **23**: 238.
26. Li ZF, Wang SW, Wang YX, Fu FX, Pan HD, Lin YH. *Chin. J. Struct. Chem.* 2002; **21**: 87.
27. Wang XH, Liu JF. *J. Coord. Chem.* 2000; **51**: 73.
28. Zhang LJ, Zhou YS, Zeng SR, Vittal JJ, You XZ. *J. Chem. Crystallogr.* 2000; **30**: 259.
29. Tian LJ, Zhou ZY. *Chem. J. Chin. Univ.-Chin.* 2002; **23**: 1231.
30. Tian LJ, Zhao B, Li F. *Synth. React. Inorg. Met.-Org. Chem.* 2002; **31**: 139.
31. Tian LJ, Zhou ZY, Zhao B, Wu WT, Yang P. *Synth. React. Inorg. Chem.* 2000; **30**: 307, 1363.
32. Tian LJ, Zhao B, Zhou ZY, Xia M, Yu W, Wang P. *Chin. Chem. Lett.* 2000; **11**: 517.
33. Tian LJ, Zhou ZY, Zhao B, Su Y, Zhang C. *Main Group Met. Chem.* 1998; **12**: 735.
34. Tian LJ, Zhou ZY, Zhao B, Yu W. *Polyhedron* 1998; **17**: 1275.
35. Tian LJ, Zhao B, Fu FX. *Synth. React. Inorg. Met.* 1998; **28**: 175.
36. Howie RA, Wardell SMSV. *Acta Crystallogr. Sect C* 2002; **58**: m220.
37. Harrison PG, King TJ, Healey MA. *J. Organometal. Chem.* 1979; **182**: 17.
38. Howie RA, Paterson ES, Wardell JL, Burley JW. *J. Organometal. Chem.* 1986; **304**: 301.
39. Jung OS, Lee YA, Jeong JH. *Bull. Korean Chem. Soc.* 1992; **13**: 404.
40. Howie RA, Wardell JL. *Acta Crystallogr. Sect C* 2001; **57**: 1041.
41. Howie RA, Wardell JL. *Acta Crystallogr. Sect C* 2000; **56**: 806.
42. Otwinowski Z, Minor W. In *Macromolecular Crystallography, Part A*, Cater CW, Sweet RM (eds). *Methods in Enzymology*, vol. 276. Academic Press: New York, 1997; 307–326.

43. Hooft RWW. COLLECT. Nonius BV, Delft, The Netherlands, 1998.
44. Blessing RH. *Acta Crystallogr. Sect A* 1995; **51**: 33.
45. Blessing RH. *J. Appl. Crystallogr.* 1997; **30**: 421.
46. Bruker SADABS, version 2.03 & SAINT, version 6.02a. Bruker AXS Inc., Madison, WI, USA, 2000.
47. Sheldrick GM. SHELXS-97. Program for the solution of crystal structures. University of Göttingen, Germany. 1997.
48. McArdle P. OSCAIL for Windows. National University of Ireland, Galway, Ieland, 2000.
49. Sheldrick GM. SHELXL-97. Program for the crystal structure refinement. University of Göttingen, Germany, 1997.
50. Spek AL. PLATON. Version of 2002. University of Utrecht, the Netherlands, 2002.
51. Farruga LJ. *J. Appl. Crystallogr.* 1997; **30**: 565.
52. Schmidt MW, Baldridge KK, Boatz JA, Elbert ST, Gordon MS, Jensen JH, Koseki S, Matsunaga N, Nguyen KA, Su SJ, Windus TL, Dupuis M, Montgomery JA. *J. Comput. Chem.* 1993; **14**: 1347.
53. Baker J, Kessi A, Delley B. *J. Chem. Phys.* 1996; **105**: 192.
54. Boatz JA, Gordon MS. *J. Phys. Chem.* 1989; **93**: 1819.
55. Burley JW, Hope P, Mack AG. *J. Organometal. Chem.* 1984; **284**: 171.
56. Desiraju GR, Steiner T. *The Weak Hydrogen Bond*. Oxford University Press: 1999.
57. Buntine MA, Hall VJ, Kosovel FJ, Tiekink ERT. *J. Phys. Chem.* 1998; **102**: 2472.
58. Frank W, Reiss GJ, Kuhn D. *Acta Crystallogr. Sect. C* 1994; **50**: 1904.
59. Janiak C, Weimann R, Gorlitz F. *Organometallics* 1997; **16**: 4933.
60. Al-Juaid SS, Al-Rawi M, Eaborn C, Hitchcock PD, Smith JD. *J. Organometal. Chem.* 1998; **564**: 215.
61. Reuter H, Eickmeier H, Puff H, Beckerman N, Hannsgen D. *Acta Crystallogr. Sect. C* 2002; **58**: m217.
62. Tse JS, Collins MJ, Lee FL, Gabe EJ. *J. Organometal. Chem.* 1986; **310**: 169.
63. Bartlett RA, Cowley A, Jutzi P, Olmstead MM, Stammler HG. *Organometallics* 1992; **11**: 2837.
64. Rocco AM, Pereira RP, Bonapace JAP, Comerlato NM, Milne BF, Wardell SMSV, Wardell JL. *Inorg. Chim. Acta* 2004; **357**: 1047.

